Preparation and Properties of Thermally Conductive Photosensitive Polyimide/Boron Nitride Nanocomposites

Tung-Lin Li, Steve Lien-Chung Hsu

Department of Materials Science and Engineering, Center for Micro/Nano Science and Technology, National Cheng-Kung University, No.1, University Road, Tainan City 701 Tainan, Taiwan, Republic of China

Received 2 June 2010; accepted 17 October 2010
DOI 10.1002/app.33631
Published online 25 February 2011 in Wiley Online Library (wileyonlinelibrary.com).

ABSTRACT: A new thermally conductive photoresist was developed. It was based on a dispersion of boron nitride (BN) nanoflakes in a negative-tone photosensitive polyimide (PSPI) precursor. 3-Mercaptopropionic acid was used as the surfactant to modify the BN nanoflake surface for the dispersion of BN nanoflakes in the polymer. The thermal conductivity of the composite films increased with increasing BN fraction. The thermal conductivity of the PSPI/BN nanocomposite was up to 0.47 W m^{-1} K^{-1} for a mixture containing 30 wt % nanosized BN filler in the polyimide matrix. Patterns with a resolution of 30 μm were obtained from the PSPI/BN nanocomposites. The PSPI/BN nanocomposites had excellent thermal properties. Their glass-transition temperatures were above 360°C, and the thermal decomposition temperatures were over 460°C. © 2011 Wiley Periodicals, Inc. J Appl Polym Sci 121: 916–922, 2011

Key words: nanocomposites; photoresists; polyimides

INTRODUCTION

Photosensitive polymer nanocomposites have versatile applications in different fields because of their unique electrical, thermal, mechanical, and optical properties. According to literature, acrylate, epoxy, and polyimide polymers have been used as the matrixes of photosensitive hybrid polymer composites with the addition of various kinds of inorganic fillers. Among them, polyimides are a class of high-performance polymers that have excellent physical and chemical properties and are widely used in microelectronic devices, such as buffer coatings, interlayer insulation, and wafer-scale packages.[1] In addition, photosensitive polyimides (PSPIs) have attracted great interest because they simplify the processing steps by preventing the use of photoresists to obtain the desired patterns.[2]

As discussed in previous reports, several fillers have been used to fabricate photosensitive polymer composites, such as silver or carbon black for the enhancement of electrical conductivity,[3–10] titanium dioxide for increasing the refractive index,[11] and montmorillonite clay and silicon dioxide for improving the mechanical and thermal properties.[12–17] Because of the demands in denser and faster circuits in electronic devices, the dissipation of heat generated in electronic components has attracted more attention and is considered an important issue to be resolved. Conventionally, alumina (Al_2O_3),[18,19] silica (SiO_2),[20,21] silicone carbide (SiC),[22] silicon nitride (Si_3N_4),[23–25] aluminum nitride (AlN),[26–28] and boron nitride (BN)[29–31] have been commonly used as thermally conductive materials in polymer matrixes. However, photosensitive polymer nanocomposites with high thermal conductivities are rarely discussed.

Here we report on the preparation and properties of a high-temperature, thermally conductive, and photosensitive nanocomposite material containing BN nanoflakes dispersed in a PSPI precursor matrix. The synthesis of the PSPI precursor, the surface modification of the BN nanofillers, and the photolithographic performance of the thermally conductive photoresist are discussed.

EXPERIMENTAL

Materials

Pyromellitic dianhydride (PMDA), 2,2′-bis(3-amino-4-hydroxyphenol) hexafluoropropane (BisAPAF), and 4,4′-diaminodiphenyl ether (4,4′-ODA) were purchased from Chriskev Co (Leawood, KS). Anhydrous *N*-methyl-2-pyrrolidone (NMP), pyridine, γ-butyrolactone (GBL), 3-mercaptopropionic acid (MPA), tetra(ethylene glycol) diacrylate, *N*-(3-dimethylaminopropyl)-*N*-ethylcarbodiimide hydrochloride, and 4-dimethylaminopyridine were obtained from Aldrich (St. Louis, MO) and were used without further

Correspondence to: S. L.-C. Hsu (lchsu@mail.ncku.edu.tw).
Contract grant sponsor: National Science Council; contract grant number: NSC-94-2120-M-006-007.

© 2011 Wiley Periodicals, Inc.

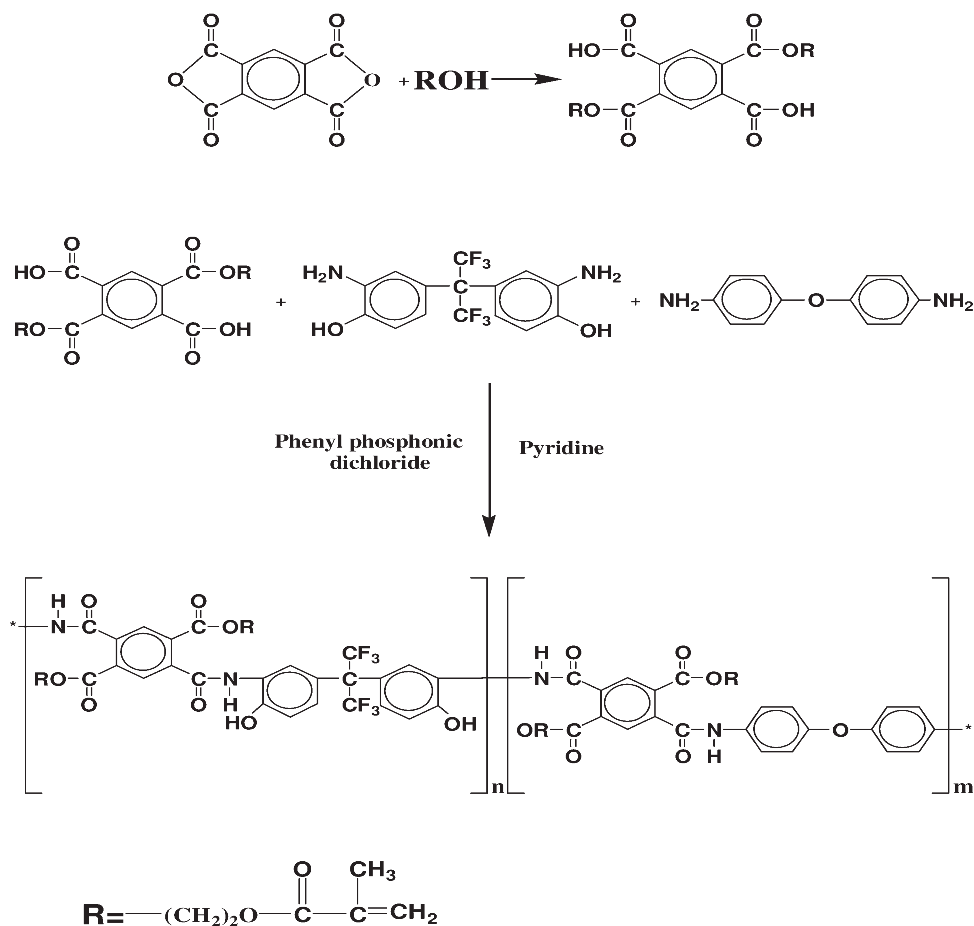

Scheme 1 Synthesis of the PMDA–BisAPAF–ODA–HEMA copoly(amic esters).

purification. 2-Hydroxyethyl methacrylate (HEMA) and hydroquinone were obtained from Acros Organics Co. (Cornwall, UK) Michler's ketone and tetramethylammonium hydroxide (TMAH) in a 25 wt % aqueous solution were purchased from Lancaster (Haverhill, MA). Tribromomethyl phenyl sulfone was obtained from TCI Co (Springfield, VA). BN nanoflakes were obtained from Shineso Co (Zhejiang, China). Its average size was 70 nm. Other chemicals and solvents were obtained commercially and were used as received.

Synthesis of the PSPI precursor: PMDA–BisAPAF–ODA–HEMA copoly(amic ester)

PMDA–BisAPAF–ODA–HEMA copoly(amic ester) was synthesized from PMDA, BisAPAF, and 4,4′-ODA in NMP by direct polymerization in the presence of phenylphosphonic dichloride as an activator, according to Scheme 1. We reported the detailed synthesis procedure in a previous article.[32] In this study, PMDA–75% BisAPAF–25% ODA–HEMA copoly(amic ester) (BisAPAF/ODA molar ratio = 75/25) was synthesized as the negative-tone polyimide precursor. The inherent viscosity was 0.43 dL/g, as measured in NMP at a concentration of 0.5 dL/g at 30°C.

Surface modification of the BN nanoflakes

To prevent the agglomeration of BN, MPA was used as the surfactant to functionalize the BN surface. BN (2 g, 83 mmol) was added to ethanol (2 L). The mixture was ultrasonicated for 20 min. Then, MPA (17.69 g, 166 mmol), *N*-(3-dimethylaminopropyl)-*N*-ethylcarbodiimide hydrochloride (38.34 g, 200 mmol), and 4-dimethylaminopyridine (12.22 g, 10 mmol) were added to the mixture (MPA/BN molar ratio = 2/1) and stirred for 24 h. The solution was centrifuged (5500 rpm) to remove the solvent and unreacted MPA molecules. The BN was washed twice with ethanol and dried at room temperature *in vacuo.*

Preparation of the PSPI/BN nanocomposites and lithographic evaluation

The thermally conductive PSPI/BN nanocomposites were prepared by the homogeneous mixing of the PSPI precursor with BN nanoflakes. A representative of the PSPI–BN10 formulation (10 wt % BN nanoflakes in the PSPI precursor) is as follows: PMDA–BisAPAF–ODA–HEMA copoly(amic ester) (1 g) was dissolved in NMP (2.33 g). To this solution, Michler's ketone (0.03 g, 3 phr), tribromomethyl phenyl

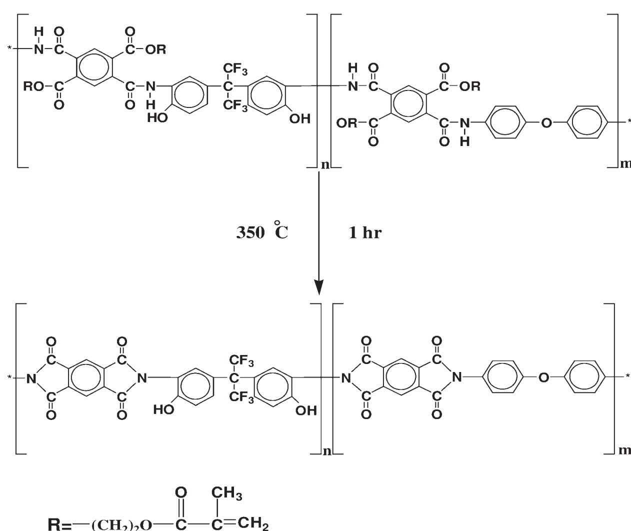

Scheme 2 PMDA–BisAPAF–ODA–HEMA copoly(amic ester) converting into PMDA–BisAPAF–ODA polyimide.

sulfone (0.08 g, 8 phr), and tetra(ethylene glycol) diacrylate (0.15 g, 15 phr) were added. The solution was filtered through a 5-μm Teflon filter. Modified BN nanoflakes (0.11 g) were added to the previous solution. The solution was stirred by a magnetic stirrer to form a homogeneous nanocomposite photoresist.

The photoresist was then spin-coated onto a silicon wafer and soft-baked on a hot plate at 90°C for 10 min to obtain a film. The thickness of the film, as measured by an Alpha-Step Profilometer (AS 500, TENCOR, Milpitas, CA), was 6–8 μm. The film was then exposed through a single-side mask aligner (OAI, 500-IR, San Jose, CA) in contact mode. The irradiation wavelength was 365 nm. The exposed film was developed in a mixed solvent developer of 2.38 wt % TMAH and GBL (TMAH/GBL ratio = 3 : 1). The required development time was dependent on the pattern geometry and BN concentration of the resist formulations. Finally, the patterns were rinsed with isopropyl alcohol and cured at 100°C for 1 h, 200°C for 1 h, and 350°C for 1 h to convert the poly(amic ester) to a polyimide, as shown in Scheme 2. We obtained the characteristic curve of the photoresist by plotting the normalized film thickness against the exposure energy.

Characterization of the PSPI/BN nanocomposite

The IR spectra were recorded on a Jasco 460 Fourier transform infrared spectrometer (Tokyo, Japan). The inherent viscosity was measured with a Cannon-Ubbelohde no. 100 viscometer (State College, PA) at a concentration of 0.5 g/dL in NMP at 30°C. The weight losses of the surfactant and the PSPI/BN were analyzed with a TA Instruments thermogravimetric analyzer TA, Q500 (New Castle, DE) at a heating rate of 10°C/min under air. The shape of the

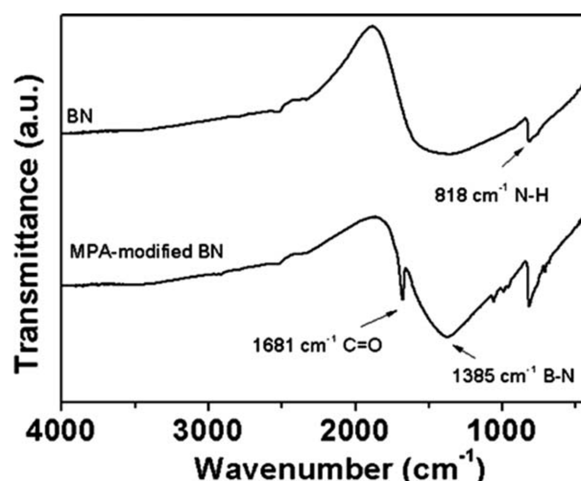

Figure 1 IR spectra of the MPA-modified BN nanoflakes.

BN nanoflakes was observed by transmission electron microscopy (JEOL, JEM-2010, Tokyo, Japan). The thermal conductivity was evaluated by a Hot-disk thermal analyzer (TPS 2500, Gothenburg, Sweden) equipped with a 30-mm diameter Kapton sensor disk. The samples were 10-mm diameter or larger disks, and the film thicknesses were 30 μm. Two identical samples were needed for each testing. One sample was placed beneath and the other was placed on the top of the sensor with an immersed heat source. Data were collected from both samples at the same time, and the reported thermal conductivity data represent the average values of both samples. The resulting resist patterns were observed by a scanning electron microscope (JEOL, JSM-6700). The in-plane coefficients of thermal expansion (CTEs) and glass-transition temperatures (T_g's) of the PSPI/BN nanocomposite membranes were determined with a TA Instruments thermal mechanical analyzer (Q400EM). The CTEs were measured with an extension probe under a 0.05-N tension force on

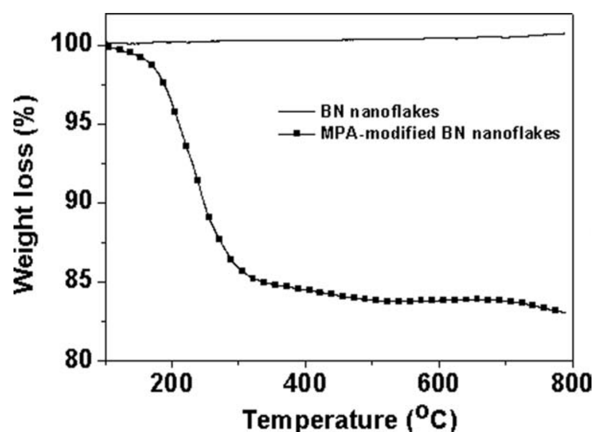

Figure 2 TGA thermograms of the untreated BN nanoflakes and surfactant-modified BN nanoflakes.

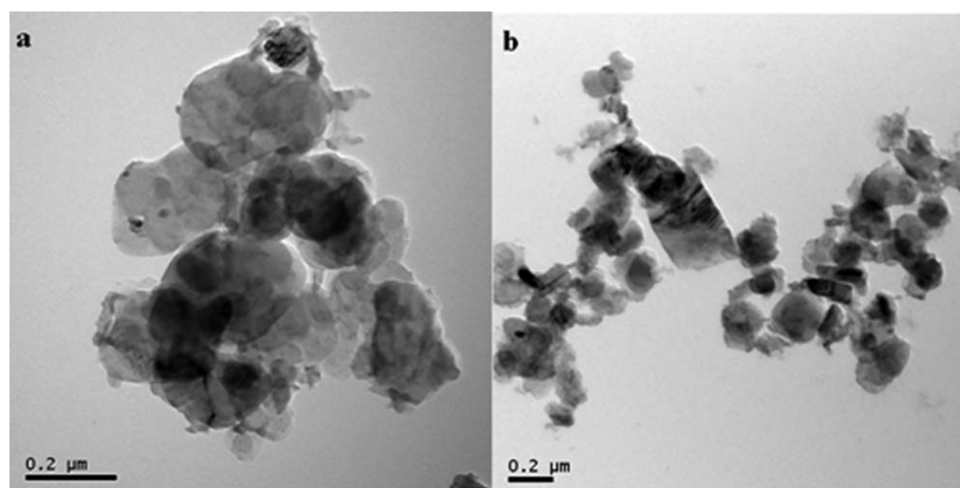

Figure 3 Transmission electron micrographs of the (a) original BN nanoflake clusters and (b) surfactant-modified BN nanoflakes dispersed in ethanol.

the films in the temperature range 100–250°C at a heating rate of 5°C/min under nitrogen.

RESULTS AND DISCUSSION

Homogeneity of the PSPI/BN nanocomposites

Various kinds of thermally conductive fillers, including SiC, diamond, Al_2O_3, AlN, and BN, have been chosen to obtain thermally conductive photosensitive composites. BN was used as the thermally conductive filler in this study because of its high thermal conductivity (up to 400 W m^{-1} K^{-1}) and relatively low dielectric constant (ca. 4).[29] Moreover, BN also exhibits excellent resistances to oxidation and chemical corrosion. However, the dispersion of the BN nanoflakes in the polymer matrix is an important issue for composite fabrication. The simple blending of the BN nanoflakes and PSPI precursor resulted in the aggregation of BN nanoflakes because of the different polarities between the organic and inorganic phases. One of the best ways to uniformly disperse the inorganic phase into a polymer matrix is to functionalize the surface of the inorganic phase with organic surfactants. MPA was used as the surfactant in this study to functionalize the BN nanoflake surface. The carboxylic acid groups of the surfactant could be used to modify the BN surface to prevent agglomeration and to enhance its compatibility with the polymer matrix.[5] The Fourier transform infrared spectra were used to investigate the MPA-modified BN particles. As shown in Figure 1, the absorption peak at 818 cm^{-1} was attributed to the out-of-plane bending absorption of the amino groups, and the absorption peak around 1385 cm^{-1} was B—N bond vibration.[33] The MPA-modified BN, with an absorption peak at 1681 cm^{-1}, could be clearly distinguished from the unmodified BN because of the carboxylic acid (C=O) group of MPA. Figure 2 shows that the MPA-modified BN nanoflakes had a 15% weight loss between 110 and 300°C compared with the unmodified BN nanoflakes. This was due to the decomposition of the surfactant. The unmodified BN nanoflakes were aggregated, and the surfactant modified BN nanoflakes were well dispersed on a nanometer scale in ethanol, as shown in Figure 3(a,b). The length of the nanoflakes was about 100 nm, and the width was about 10 nm.

Table I summarizes the qualitative solubility of the poly(amic ester) and the PSPI/BN nanocomposites. Because of the excellent solubility of the poly(amic ester), it was easy to prepare a high-solids-content photoresist for photolithographic processing. The PSPI/BN nanocomposites showed good chemical resistance for several organic solvents.

Lithographic evaluation of the PSPI/BN nanocomposites

Because of the incorporation of BN fillers into the PSPI matrix, the lithographic behavior of PSPI was

TABLE I
Solubility of Poly(amic ester), PSPI, and PSPI/BN Nanocomposites

	Solubility		
Solvent	Poly(amic ester)	PSPI	PSPI–BN10
NMP	+	−	−
DMAc	+	−	−
THF	+	−	−
Toluene	+	−	−
$CHCl_3$	+	−	−
Acetone	+	−	−
Methanol	−	−	−

DMAc, dimethylacetamide; THF, tetrahydrofuran, +, soluble; −, insoluble.

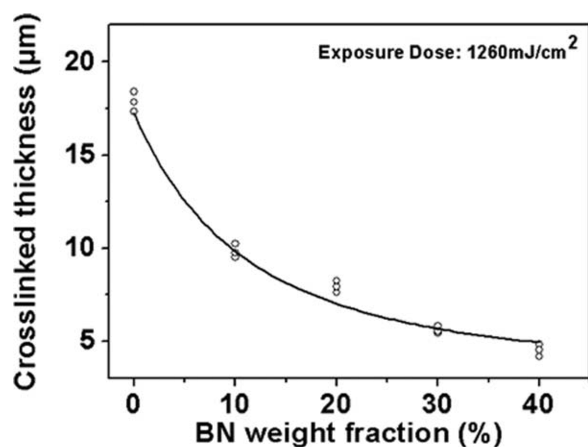

Figure 4 Crosslinked thickness of the PSPI/BN nanocomposites versus the BN nanoflake weight fraction. The exposure dose was 1260 mJ/cm^2.

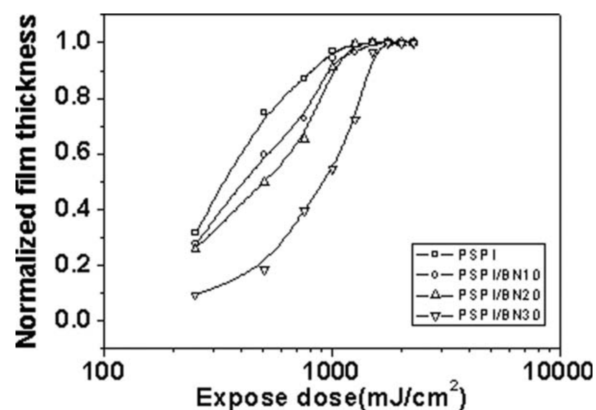

Figure 5 Characteristic exposure curves of the PSPI and PSPI/BN nanocomposites.

changed because the BN nanoflakes reflected the irradiation wavelength at 365 nm. Therefore, the BN nanoflakes had a great influence on the photocrosslinking of the negative-tone PSPI precursor. The precursor became insoluble in the developer after exposure to UV light because of the crosslinking of photosensitive acrylate groups in the polymer. Figure 4 shows the changes in the crosslinked PSPI/BN thickness versus the BN weight fraction. The crosslinked thickness was measured by the surface profilometry of the patterns on the silicon wafer after development in the developer and cured at 350°C. The crosslinked thickness decreases with increasing BN weight fractions. At an exposure dose of 1260 mJ/cm^2, the crosslinked thickness for a BN weight fraction of 10% was about 10 μm. The reduction of the crosslinked thickness of the PSPI/BN photoresist compared to the pure PSPI was due to the reflection of light by the BN nanoflakes. Such behavior was reported by previous studies, which had added inorganic nanoparticles in photoresists.[3,4,16]

Because of the reflectivity of the BN fillers, the lithographic properties showed an obvious difference between the pure PSPI and PSPI/BN photoresists. Figure 5 shows the characteristic exposure curves of the pure PSPI and BN/PSPI, which contained a 30% weight fraction of BN fillers. The contrast at a 0.5 gel fraction ($\gamma^{0.5}$) and the sensitivity at the 0.5 gel fraction ($D^{0.5}$) of pure PSPI were 1.27 and 338 mJ/cm^2, respectively. For the PSPI/BN, which contained a 30% BN weight fraction, the contrast ($\gamma^{0.5}$) was 1.19, and the sensitivity ($D^{0.5}$) was 913 mJ/cm^2. Patterns with a resolution of 30 μm were obtained in 6 μm thick films with various BN weight fractions of PSPI/BN, as shown in Figure 6.

Thermal conductivity

Compared with other thermally conductive fillers, BN is a softer filler and can attain a higher packing density at a low filler content. Lee et al.'s[34] study also confirmed that BN fillers have a maximum packing fraction below 30 vol % (ca. 68 wt %) that can form a thermally conductive network when compared to other fillers. Hence, the BN filler was the best candidate for fabricating the thermally conductive composite films at low filler contents. Figure 7 shows the thermally conductivity values of the PSPI/BN composite films with nanosized BN particles, as measured by the Hotdisk equipment. The

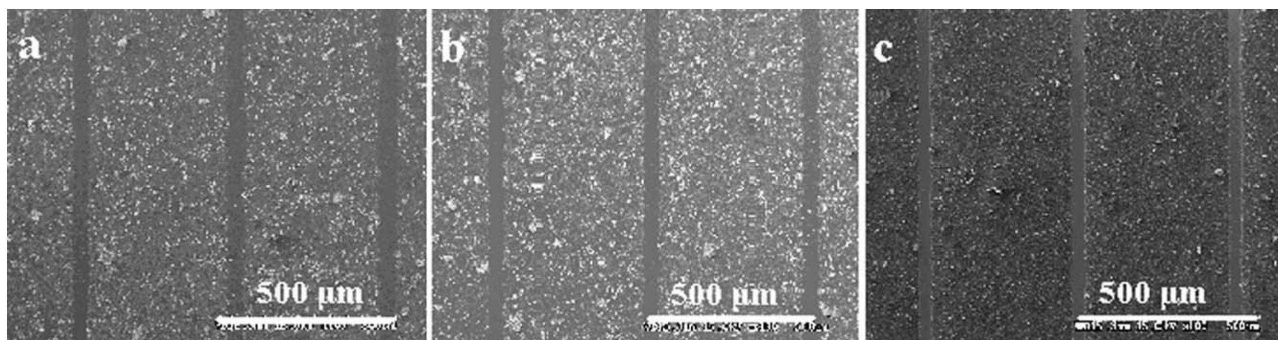

Figure 6 Scanning electron micrographs of the PSPI/BN nanocomposites with different BN weight fractions: (a) 10, (b) 20, and (c) 30%.

thermal conductivity of the composite films increased with increasing BN fraction. The PSPI/BN composite films showed the highest thermal conductivity of 0.47 W m^{-1} K^{-1} at a 30 wt % BN content, as shown in Figure 7. This thermal conductivity value was about 2.8 times higher than that of the PSPI matrix. The high thermal conductivity could be explained by the nanosized BN particles incorporated into the polyimide film; this formed a random conductive bridge or network to release the excess heat. The PSPI/BN composite films with high thermal conductivity could have great potential for use as heat-dissipative materials in microelectronic components.

Thermal properties of the PSPI/BN nanocomposites

The thermal properties of the PSPI/BN nanocomposites are summarized in Table II. The T_g values of the PSPI/BN nanocomposites were higher than that of the parent PSPI. This indicates that the BN fillers could increase the T_g of polymers. CTE of the PI/BN composite films was also crucial to prevent the mismatch with other electronic components, such as copper and aluminum (16–23 μm m^{-1} °C^{-1}). The linear CTEs for the PSPI/BN were 32–35 μm m^{-1} °C^{-1}. They were slightly lower than that of the parent PSPI (38 μm m^{-1} °C^{-1}) because of the increment of the inorganic BN contents. This indicated that the high BN filler loading and nanosize BN particles could restrain the movement of the polymer chains during the increase of temperature. From thermogravimetric analysis (TGA), the PSPI/BN nanocomposites showed excellent thermal and thermooxidative stabilities. Their 5% weight loss temperatures were up to 460°C in air. From TGA in air, the residual weight percentages of the PSPI/BN nanocomposites above 700°C were close to the BN contents in the PSPI matrix.

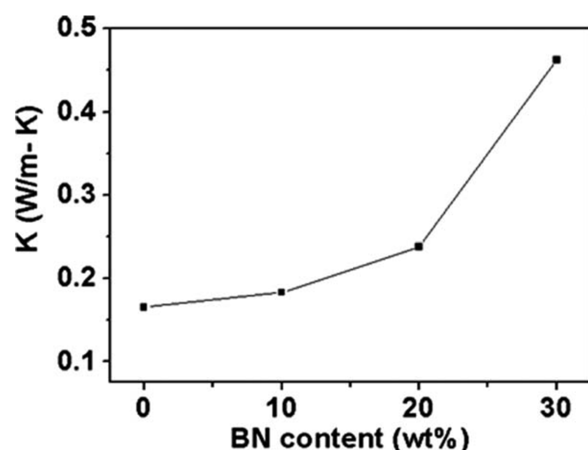

Figure 7 Thermal conductivity (K) of PSPI/BN nanocomposites versus BN weight fraction.

TABLE II
Thermal Properties of the PSPI/BN Nanocomposites

	T_g[a]	CTE (μm m^{-1}°C^{-1})[b]	$T_{5\%}$ (°C)[c]	Residue
PSPI	362	38	460	0
PSPI/BN10	371	35	461	10.2
PSPI/BN20	372	33	466	19.1
PSPI/BN30	371	32	474	33.2

[a] Identified by thermal mechanical analysis.
[b] Measured by thermal mechanical analysis in the temperature range 100–250°C.
[c] Temperature of 5% weight loss, as determined by TGA.

CONCLUSIONS

A thermally conductive photoresist was prepared from surface-modified BN nanoflakes embedded in a negative-tone PSPI. The composites became highly thermally conductive when the nanosized BN particles were added to the insulating photosensitive polymer matrix. This phenomenon appeared when the BN weight fraction was sufficient to form the thermally conductive path to dissipate the generated heat. The PSPI/BN photoresist containing 30 wt % BN showed a $D^{0.5}$ of 913 mJ/cm^2 and a contrast of 1.19 in a 6 μm thick film. Patterns with a resolution of 30 μm were obtained from this composition. Because of the excellent thermal properties, the PSPI/BN nanocomposites have the potential for use in high-temperature microfabrication of heat-dissipative components in the microelectronics industry.

We also thank Y. K. Han at the Department of Chemical and Materials Engineering of National Kaohsiung University of Applied Science, Taiwan, for his kind help in the thermal conductivity measurement.

References

1. Ghosh, M. K.; Mittal, K. L. Polyimides: Fundamentals and Applications; Marcel Dekker: New York, 1996.
2. Horie, K.; Yamashita, T. Photosensitive Polyimides, Fundamentals and Applications; Technomic: Lancaster, PA, 1995.
3. Jiguet, S.; Bertsch, A.; Hofmann, H.; Renaud, P. Adv Funct Mater 2005, 15, 1511.
4. Jiguet, S.; Bertsch, A.; Hofmann, H.; Renaud, P. Adv Eng Mater 2004, 6, 719.
5. Li, T. L.; Hsu, S. L. C. J Polym Sci Part A: Polym Chem 2009, 47, 1575.
6. Ketkar, S. A.; Umarji, G. G.; Phatak, G. J.; Ambekar, J. D.; Rao, I. C.; Mulik, U. P.; Amalerkar, D. P. Mater Sci Eng B 2006, 132, 215.
7. Ketkar, S. A.; Umarji, G. G.; Phatak, G. J.; Ambekar, J. D.; Mulik, U. P.; Amalerkar, D. P. Mater Chem Phys 2006, 96, 145.
8. Umarji, G. G.; Ketkar, S. A.; Phatak, G. J.; Giramkar, V. D.; Mulik, U. P.; Amalerkar, D. P. Microelectron Reliab 2005, 45, 1903.
9. Hauptman, N.; Zveglic, M.; Macek, M.; Gunde, M. K. J Mater Sci 2009, 44, 4625.

10. Mionic, M.; Jiguet, S.; Judelewicz, M.; Forro, L.; Magrez, A. Phys Status Solidi B 2009, 246, 2461.
11. Liu, L.; Lu, Q.; Yin, J.; Qian, X.; Wang, W.; Zhu, Z.; Wang, Z. Mater Chem Phys 2002, 74, 210.
12. Liang, Z. M.; Yin, J.; Wu, J. H.; Qiu, Z. X.; He, F. F. Eur Polym J 2004, 40, 307.
13. Wang, Y. W.; Yen, C. T.; Chen, W. C. Polymer 2005, 46, 6959.
14. Jiguet, S.; Judelewicz, M.; Mischler, S.; Hofmann, H.; Bertsch, A.; Renaud, P. Surf Coat Tech 2006, 21, 2289.
15. Zhang, A. P.; He, S.; Kim, K. T.; Yoon, Y. K.; Burzynski, R.; Samoc, M.; Prasad, P. N. Appl Phys Lett 2008, 93, 203509.
16. Jiguet, S.; Bertsch, A.; Judelewicz, M.; Hofmann, H.; Renaud, P. Microelectron Eng 2006, 83, 1966.
17. Lee, C. K.; Don, T. M.; Lai, W. C.; Chen, C. C.; Lin, D. J.; Cheng, L. P. Thin Solid Films 2008, 516, 8399.
18. Shimazaki, Y.; Hojo, F.; Takezawa, Y. Appl Phys Lett 2008, 92, 133309.
19. Bujard, P.; Kuhnlein, G.; Ino, S.; Shiobara, T. IEEE Trans Compon Packag Manuf Technol Part A 1994, 17, 527.
20. Lee, W. S.; Yu, J. Diamond Relat Mater 2005, 14, 1647.
21. Gonon, P.; Sylvestre, A.; Teysseyre, J.; Prior, C. J Mater Sci Mater Electron 2001, 12, 81.
22. Hussain, M.; Oku, Y.; Nakahira, A.; Niihara, K. Mater Lett 1996, 26, 177.
23. Zhou, W.; Wang, C.; Ai, T.; Wu, K.; Zhao, F.; Gu, H. Compos Part A 2009, 40, 830.
24. He, H.; Fu, R.; Shen, Y.; Han, Y.; Song, X. Compos Sci Technol 2007, 67, 2493.
25. Riley, F. L. J Am Ceram Soc 2000, 83, 245.
26. Yu, S.; Hing, P.; Hu, X. Compos Part A 2002, 33, 289.
27. Kume, S.; Yamada, I.; Watari, K.; Harada, I.; Mitsuishi, K. J Am Ceram Soc 2009, 92, S153.
28. Lee, E. S.; Lee, S. M.; Shanefield, D. J.; Cannon, W. R. J Am Ceram Soc 2008, 91, 1169.
29. Huang, M. T.; Ishida, H. J Polym Sci Part B: Polym Phys 1999, 37, 2360.
30. Ishida, H.; Rimdusit, S. Thermochim Acta 1998, 320, 177.
31. Hill, R. F.; Supancic, P. H. J Am Ceram Soc 2002, 85, 851.
32. Hsu, S. L. C.; Fan, M. H. Polymer 2004, 45, 1101.
33. Sainabury, T.; Ikuno, T.; Okawa, D.; Pacile, D.; Frechet, J. M. J.; Zettl, A. J Phys Chem C 2007, 111, 12992.
34. Lee, G. W.; Park, M.; Kim, J.; Lee, J. I.; Yoon, H. G. Compos Part A 2006, 37, 727.